BMC Cancer

RESEARCH

Open Access

Fucosyltransferase 11 restrains ferroptosis via upregulation GPX4 expression in gastric cancer

Bingbing Zhang[1†], Yali Chen[1†], Xuezhou Gu[2†], Yu Zheng[3] and Zhong Hua Jiang[1*]

Abstract

Ferroptosis is a novel iron-dependent type of programmed cell death that is characterized by the oxidation of lipids by divalent iron ions to produce lipid peroxides, which leads to cell death. Fucosyltransferase 11 (FUT11) is highly expressed in most tumors and is involved in tumorigenesis. However, there have been few studies regarding the relationship between FUT11 and ferroptosis. In this study, we found that FUT11 expression was abnormally high in gastric cancer (GC) cells and that the prognosis of patients with GC and high expression of FUT11 was poor. FUT11 expression was significantly correlated with the TNM stage of GC.Specific knockdown of FUT11 significantly inhibited the proliferation of GC cells, reduced the abundance of the key anti-ferroptotic protein glutathione peroxidase 4(GPX4), induced lipid peroxidation and ferroptosis in GC cells, and inhibited the proliferation of these cells. The overexpression of GPX4 reduced the inhibitory effect of FUT11 on GC cells. In addition, the knockdown of FUT11 significantly inhibited GC tumor growth in mice, and this inhibitory effect was reduced by the overexpression of GPX4. In conclusion, we have shown that FUT11 promotes GC progression by targeting GPX4, thereby inhibiting ferroptosis in GC cells. These findings suggest that FUT11 is a potential therapeutic target for GC.

Keywords FUT11, Gastric cancer, GPX4, Ferroptosis

Introduction

Gastric cancer (GC) is the fifth most common malignancy worldwide and the fourth most common cause of cancer-related death [1]. Owing to the atypical early symptoms of GC and the low prevalence of screening, the disease is frequently diagnosed when it is at an advanced stage [2]. A combination of surgery and perioperative radiotherapy, chemotherapy, or biotargeting therapy can prolong the survival and improve the quality of life of patients. Although the treatment of GC is evolving, patients with advanced GC still have a poor prognosis and there are high risks of recurrence and metastasis following surgery [3]. Therefore, it is necessary to facilitate the early diagnosis of GC and identify new targeted therapies.

†Bingbing Zhang, Yali Chen and Xuezhou Gu contributed to the work equally and should be regarded as co-first authors.

*Correspondence:
Zhong Hua Jiang
jiangzhonghua1982@163.com
[1]Department of Gastroenterology, The Yancheng Clinical College of Xuzhou Medical University, The First People's Hospital of Yancheng, The Yancheng Clinical Medical College of Jiangsu University, Yancheng, Jiangsu 224006, China
[2]Department of General Surgery, Sheyang People's Hospital, Yancheng, Jiangsu 224006, China
[3]Department of Laboratory Medicine, The Yancheng Clinical College of Xuzhou Medical University, The First People's Hospital of Yancheng, The Yancheng Clinical Medical College of Jiangsu University, Yancheng, Jiangsu 224006, China

Fucosyltransferases are a class of biosynthetic enzymes that are involved in fucoidan synthesis and catalyze the transfer of L-fucose from the donor substrate guanosine diphosphate β-L-fucose to various glycoreceptor substrates. To date, 13 FUTs have been identified in humans, and they are closely associated with tumor development, apoptosis, invasion, and platinum resistance [4–7]. FUT11 is a member of this family and promotes α-1,3 fucose synthesis and terminal fucosylation [8]. Previous studies have shown that FUT11 is closely associated with the development of cancer. Furthermore, high expression of FUT11 is a marker of poor prognosis in patients with renal and gynecologic cancers [9, 10]. It is also an important regulator of the proliferation, migration, and apoptosis of GC cells [11], and therefore it can be used to aid the diagnosis and in determining the prognosis of GC. Consequently, it is important to better characterize the mechanisms of its effects in GC.

In recent years, fucosylation has been found to promote CD4 T cell-mediated anti-tumor immunity by enhancing the antigen presentation function of HLA-DRB1. IFN-γ released by CD4 T cells inhibits SLC7A11 expression in tumor cells, reduces cystine uptake, leads to GSH depletion and GPX4 inactivation, thereby promoting ferroptosis [12].In addition, Deng et al. found that fucosylation of TLR4 may enhance its signaling and promote ROS production. ROS accumulation can catalyze lipid peroxidation via the Fenton reaction, triggering ferroptosis [13].

Ferroptosis is a novel iron- and reactive oxygen species (ROS)-dependent form of regulated cell death that differs from apoptosis, necrosis, and autophagy. Unlike with other types of cell death, ferroptosis is characterized by a reduction in mitochondrial volume, an increase in the density of mitochondrial membranes, a reduction in the number of mitochondrial crests, and rupture of the outer mitochondrial membrane [14, 15]. A large number of previous studies have shown that ferroptosis inhibits the growth and proliferation of liver, colorectal, gastric, ovarian, prostate, breast, and lung cancers [16–22]. However, the relationship between FUT11 and ferroptosis and its role in GC have not been previously characterized.

Glutathione peroxidase (GPX4, PHGPx), is the only enzyme that can reduce the lipid hydroperoxide content of biofilms, and the GSH–GPX4 antioxidant system plays an important role in the protection of cells against ferroptosis. Cells with low GPX4 expression have been shown to be more sensitive to ferroptosis, whereas high GPX4 expression inhibits ferroptosis. For example, Lu et al. found that KLF2 inhibits ferroptosis by increasing the expression of GPX4 and promoting the migration and invasiveness of renal cell carcinoma [23]. CST1 inhibits ferroptosis by reducing the ubiquitination of GPX4 and improving the stability of GPX4 protein, thereby promoting EMT and GC cell metastasis [24]. Finally, miR-221-3p inhibits ferroptosis in GC cells by reducing ATF3 expression, which in turn inhibits the transcription of HRD1 and GPX4 [25]. Therefore, GPX4 plays an important role in the progression of cancer, and its role in GC is worthy of further study.

In the present study, we show that the expression of FUT11 is associated with the proliferation of GC cells and that the knockdown of FUT11 promotes ferroptosis by reducing the expression of GPX4. Thus, FUT11 may represent a novel target for the therapy of GC.

Materials and methods

GEPIA data analysis

We used the interactive analytical platform GEPIA (http://gepia2.cancer-pku.cn/), which is based on pub lic databases such as TCGA and GTEx, to compare the expression of FUT11 in tissue affected by GC and adjacent non-cancerous tissue. Furthermore, we conducted Kaplan–Meier survival to analyze the prognosis of the included patients and performed gene correlation analysis.

Human GC tissue

Sections of tissue affected by GC were collected by the Pathology Department of Yancheng Clinical College of Xuzhou Medical University (Yancheng, China) between June 1, 2021 and August 1, 2022. GC-affected and adjacent non-cancerous tissue samples were obtained from patients with histologically confirmed gastric adenocarcinoma between June 30, 2023 and February 1, 2024. All of the patients provided their informed consent to participate in the study, which was approved by the Ethics Committee of Yancheng Clinical College, Xuzhou Medical University(2023-K-095).

Patients and Follow-up

For this investigation, a cohort consisting of 80 patients who underwent subtotal gastrectomy for radical treatment between 2018 and 2023 was recruited from the First People's Hospital of Yancheng City, Jiangsu Province, China. Demographic details of all patients, including name, gender, hospitalization number, wax block number, and operation date, along with their clinical and pathological data (tumor location, differentiation grade, and TNM staging), were obtained from the hospital's medical record system. The TNM stage of each patient was assigned according to the NCCN guidelines (2021 edition). Follow-up assessments were conducted at six-month intervals to document recurrence, metastasis, and the survival status of each patient. In accordance with the principles of the Helsinki Declaration, informed consent was obtained from all individuals.

Cell lines and culture

The normal human gastric mucosal epithelial cell line GES-1 and the GC cell lines HGC-27, MKN-45, MGC-803, and AGS were purchased from Fuheng Biology (Shanghai, China) in 2023. These cells were cultured in RPMI 1640 or DMEM medium (KeyGENbio, Jiangsu, China) containing 10% fetal bovine serum (FBS, ExCell, Jiangsu, China), 100 U/mL penicillin, and 100 U/mL streptomycin at 37℃ in air containing 5% CO_2. These cell lines were authenticated through short tandem repeat profiling before use and were found to be free of mycoplasma contamination.

Plasmids and transfection

The plasmids and lentivirus used for FUT11 knockdown (Sh-FUT11) and GPX4 overexpression (OE-GPX4) were provided by GeneChem Co (Shanghai, China). The sequence of Sh-FUT11 was CACTGCCATGATCC ACAACAA. OE-GPX4 was performed using a lentivirus constructed using the Ubi-MCS-CBh-gcGFP-IRES-puromycin vector (GeneChem Co). The knockdown and overexpression of the target proteins were verified using western blotting and real-time -quantitative PCR.

Real-time -quantitative PCR(RT-qPCR)

RNA was extracted from cells/tissues using TRIzol reagent (R701-01 Vazyme, Nanjing, China) and the concentrations of the samples were quantified by measuring the absorbance at 260 nm. Subsequently, the purified RNA was reverse transcribed to cDNA using HiScript II Q RT SuperMix (R223, Vazyme). RT-qPCR was performed using 2×ChamQ Universal SYBR qPCR Master Mix (Q711, Vazyme). The relative mRNA expression of the target genes was calculated using the $2^{-\Delta\Delta CT}$ method, with *β-actin* as the reference gene. The primer sequences used were as follows:

β-actin: F: GTCATTCCAAATATGAGATGCGT R: GCT ATCACCTCCCCTGTGTG.

FUT11:F: GAGATTCCTGAGAATGACAGTTGG R: TT GTGGATCATGGCAGTGAGA.

GPX4:F: GAGGCAAGACCGAAGTAAACTAC; R: CC GAACTGGTTACACGGGAA;

SLC7A11:F: TGGGACAAGAAACCCACCTG R: TCCC TATTTTGTGTCTCCCCTTG.

SLC3A2:F: TGAATGAGTTAGAGCCCGAGA R: GTCT TCCGCCACCTTGATCTT.

ACSL4:F: TTTTTGCGAGCTTTCCGAGTG R: GCCG ACAATAAAGTACGCAAATG.

TFRC: F: AGGACGCGCTAGTGTTCTTC R: TGCTGT CCAGTTTCTCCGAC.

Cell viability assessment

Cell viability was assessed using a Cell Count Kit (CCK)-8 assay. GC cells were seeded into 96-well plates at 3×10^3 cells per well and incubated at 37 °C for 0, 24, 48, or 72 h. At each time point, 10 μl of CCK-8 reagent (Abbkine, Wuhan, China) was added to each well, then the cells were incubated for a further 2 h at the same temperature. The absorbance of each well was then measured at 450 nm using a multi-functional microplate reader (Thermo Fisher Scientific, Waltham, MA, USA).

Colony formation assay

Colony formation rate is an indicator of cellular proliferation. Cells were seeded into six-well plates at a density of 1,000 cells per well and cultured in complete medium for 10 days until colonies were visible to the naked eye. After fixing the cells with 4% paraformaldehyde, staining with crystal violet, and rinsing with tap water, photographs were obtained and the colony sizes were analyzed using Image J software (NIH, Bethesda, MD, USA).

Western blot analysis

Cells and tissues were lysed in RIPA buffer (Servicebio, Wuhan, China), then the protein concentrations of the lysates were measured using the BCA method (Beyotime Bio, P0012S, Jiangsu, China). The lysates were then mixed with 5× loading buffer at a ratio of 4:1, incubated at 95 °C for 10 min, and then separated on SDS-PAGE gels. After the transfer of the proteins onto PVDF membranes (Millipore, Burlington, MA, USA) and blocking with 10% skim milk for 2 h, target proteins were identified using anti-FUT11 (1:500, 17175-AP, Proteintech, Wuhan, China), anti-GPX4 (1:1,000, ET1706-45, Huaanbio, Hangzhou, China), and anti-4-HNE (1:500, A24456, ABclonal, Wuhan, China) antibodies; and anti-β-actin (1:10,000, AC006, ABclonal) and anti-GAPDH (1:10,000, AC002, ABclonal) were used to detect the proteins used as loading controls. HRP-conjugated goat anti-rabbit (AS014) and anti-mouse (AS003) IgG (1:10,000, ABclonal) secondary antibodies were used. Specific bands were visualized using an enhanced chemiluminescent chromogenic substrate (Abbkine, Wuhan, China) and quantified using a Molecular Imager ChemiDoc imaging system (Bio-Rad, Hercules, CA, USA).

Immunohistochemical staining

Tissue samples were fixed in formalin, embedded in paraffin, and sectioned. Subsequently, the sections were deparaffinized, hydrated, and subjected to heat-induced antigen retrieval. Afterwards, 3% hydrogen peroxide was added dropwise to quench endogenous peroxidase activity, then the sections were blocked with 3% goat serum and incubated overnight at 4 °C with the following antibodies: anti-FUT11 (1:50, 17175-AP, Proteintech), anti-GPX4 (1:500, ET1706-45, Huaan Biotechnology, Hangzhou, China), or anti-4-HNE (1:100, A24456, Abclonal). The sections were then incubated

with HRP-conjugated rabbit secondary antibody (1:200, G1215, Servicebio, Guangdong, China) for 2 h at room temperature, stained using 3,3-diaminobenzidine tetrahydrochloride, counter-stained with hematoxylin, sealed with neutral resin, and examined under a light microscope (Hitachi HT7700, Tokyo, Japan).

Immunofluorescence (IF) staining

Cells seeded onto coverslips were fixed with 4% paraformaldehyde, permeabilized with 0.1% Triton X-100, and then blocked with 5% BSA. They were then incubated overnight at 4 °C with Ki67 antibody (1:1,000, 27309-1-AP, Proteintech) or 4-HNE antibody (1:200, A24456, Abclonal). Subsequently, the cells were incubated with CoraLite594-conjugated goat anti-rabbit IgG (1:250, SA00013-4, Proteintech), the secondary antibody, for 1 h, washed three times with PBS, and their nuclei were stained with DAPI. Images were captured using a fluorescence microscope (Hitachi HT7700).

In vivo mouse experiments

Six-week-old male BALB/c nude mice purchased from the Comparative Medical Center of Yangzhou University were randomly divided into four groups ($n = 5$ per group), and injected with 5×10^6 cells (100 µl PBS + 100 µl Matrigel-356234, Corning, Corning, NY, USA) in the left side of the armpits. Tumor size was measured every 3 days, and 1 month later, the mice were euthanized by carbon dioxide inhalation for tumor size assessment. Calipers were used to measure the tumor diameters, and their volumes were calculated using $V = (A \times B^2)/2$, where A = tumor long axis and B = tumor short axis. All the animal procedures were conducted in accordance with the guidelines of the Ministry of Science and Technology of the People's Republic of China (published September 30, 2006) for animal welfare, and were approved by the Medical Laboratory Animal Ethics Committee of Jiangsu Medical Vocational College(SYLL-2023-706).

Assay of intracellular ROS

To quantify their ROS content, cells were treated with 10 µmol/L 2,7-dichlorodihydrofluorescein diacetate (KGAF019, KeyGENbio, Jiangsu, China) for 30 min at 37℃. Every 5 min, the suspension was gently inverted to ensure thorough contact between the probe and the cells. At the end of this period, the oxidation of intracellular fluorophores was measured by flow cytometry (KeyGENbio). The results are expressed as the mean fluorescence intensity.

Malondialdehyde (MDA) assay

After collecting 5×10^6 cells, they were washed with cold PBS, centrifuged, and the supernatant was discarded. Subsequently, 1 mL of pre-chilled Extraction Buffer was added, and the cells were sonicated in an ice bath for 5 min. After centrifugation at 13,000 × *g* and 4 °C for 10 min, the supernatant was collected, then the concentration of the lipid peroxidation product MDA was measured according to the manufacturer's instructions (Abbkine, KTB1050). The absorbance of the solutions was read using a multifunctional microplate reader (Thermo Fisher Scientific).

Transmission electron microscopy (TEM)

HGC-27 and MKN-45 cells were collected by low-speed centrifugation and fixed in electron fixation solution containing 2.5% glutaraldehyde (G1102, Servicebio). After post-fixation using 1% osmium tetroxide and dehydration, the samples were embedded in epon resin, stained with uranyl acetate, and examined using a transmission electron microscope (Hitachi HT7700, Japan).

Data analysis

Prism v.9 (GraphPad Software, La Jolla, CA, USA) was used for the statistical analyses. Unpaired *t*-tests were used for comparisons between two groups, and one-way or two-way analysis of variance (ANOVA) was used for comparisons of three or more groups.The survival curves were estimated by Kaplan-Meier analysis, and *P* values were calculated by log rank test. Univariate Cox proportional hazards regressions were applied to estimate the individual hazard ratio (HR) for the overall survival. The HR with a 95% confidence interval (CI) was measured to estimate the hazard risk of individual factors. Differences were considered to be statistically significant when $P < 0.05$.

Results

FUT11 is overexpressed in GC-affected tissue

To investigate the role of FUT11 in the pathogenesis of GC, we conducted a bioinformatic analysis of TCGA and GTEx data using GEPIA. We found that FUT11 was expressed at a significantly higher level in GC tissue ($n = 408$) than in non-tumor gastric tissue ($n = 211$) and was closely associated with overall survival. Patients with GC and high expression of FUT11 had a lower overall survival rate,$P < 0.05$ (Fig. 1A, B). We next conducted an immunohistochemical analysis of tumor tissue and adjacent normal tissue from patients with GC, and found a specific upregulation of FUT11 expression in the former (Fig. 1C). Subsequent analysis revealed that both the protein and mRNA expression of FUT11 was higher in the GC cell lines HGC-27, MGC803, and MKN-45 than in normal gastric mucosal epithelial cells (GES-1) (Fig. 1E and F). On the basis of the cell tumorigenicity and the expression of FUT11, we selected the HGC-27 and MKN-45 cell lines for further study.

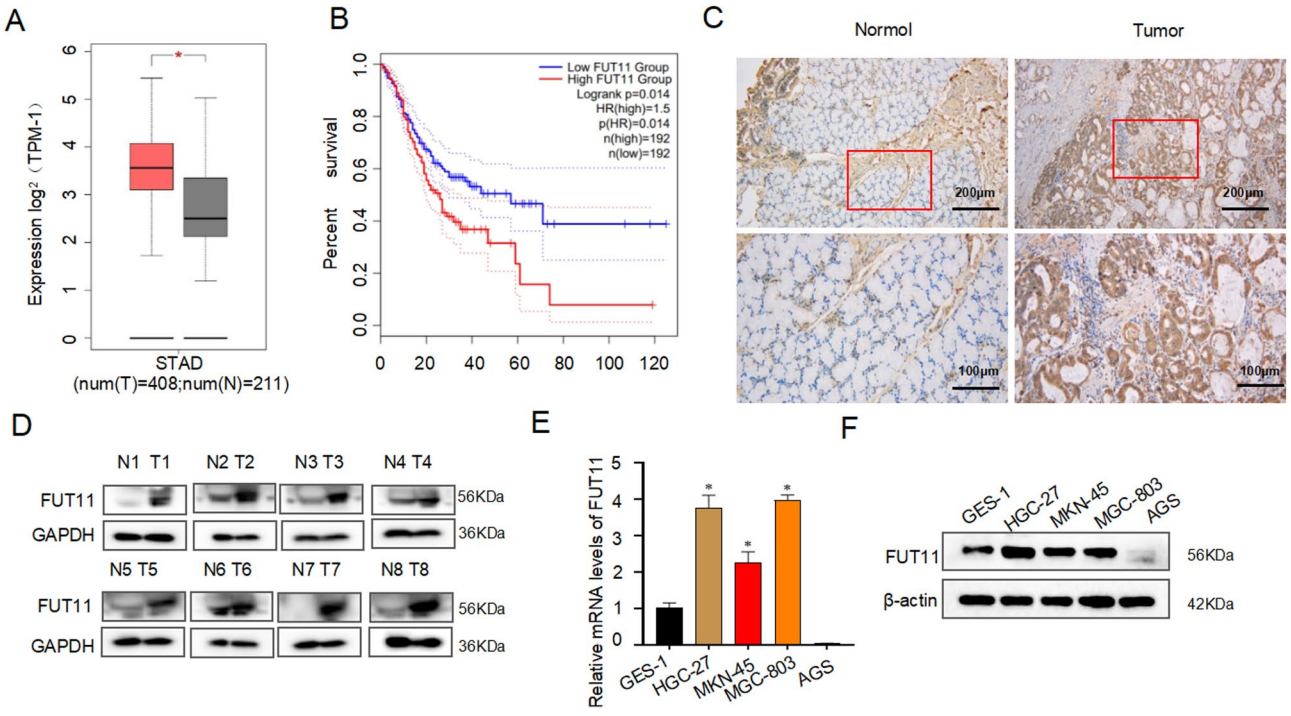

Fig. 1 FUT11 is highly expressed in the tissues of patients with GC. **A**, **B.** An analysis using GEPIA showed that the expression of FUT11 in GC-affected tissue was significantly higher than in non-tumor gastric tissue, and that it was closely associated with prognosis. $p < 0.05$. **C.** Immunohistochemical analysis showed differential expression of FUT11 in GC and adjacent normal tissue. **D.** Western blot analysis revealed differential expression of FUT11 protein in GC and adjacent normal tissue. **E**, **F** Expression of FUT11 protein and mRNA in normal gastric epithelial cells (GES-1) and four GC cell lines (HGC-27, MGC-803, MKN-45, and AGS), determined using western blotting and RT-qPCR. * $p < 0.05$ *versus* the corresponding control

FUT11 increasingly expressed in GC tissues and exhibited major clinical significance

We enrolled 80 GC patients who underwent surgery at our hospital and assessed FUT11 expression in their cancer tissues. Subsequently, we evaluated the association between FUT11 protein levels and the clinical outcomes of these patients. Notably, patients with elevated FUT11 expression exhibited a shorter survival time compared to those with lower FUT11 expression (Fig. 2A).Based on the results of the Cox analysis, an elevated expression of FUT11 showed a significant association with patient outcome in the univariate Cox analysis (Fig. 2B). Furthermore, factors such as FUT11 expression, differentiation grade, and TNM stage were found to be associated with the survival prognosis of GC patients. Importantly, after adjusting for grade and stage, multivariate Cox regression analysis demonstrated that increased FUT11 expression in GC served as a statistically significant predictor of patient survival prognosis.Using immunohistochemical results, we categorized the patients into FUT11-negative (-), weak positive (+), medium positive (++), and strong positive (+++) groups. Clinical analysis indicated that FUT11 expression was significantly correlated with the TNM stage of GC (Fig. 2C). These findings underscore the significant relationship between FUT11 and a poor prognosis in GC patients, identifying FUT11 as an important predictor of GC prognosis. They provide a new perspective for evaluating GC prognosis and developing targeted treatment strategies.

Inhibition of the expression of FUT11 reduces the proliferation of GC cells

The above results indicate that FUT11 is highly expressed in GC. To investigate the effects of FUT11 in GC cells, we used shRNA to specifically knock down FUT11 in HGC-27 and MKN-45 cells, then western blotting and RT-qPCR were used to assess the efficiency of the knockdown (Fig. 3A–C). Using a CCK-8, we found that knocking down FUT11 inhibited the proliferation of HGC-27 and MKN-45 cells (Fig. 3D). Furthermore, inhibiting the expression of FUT11 in HGC-27 and MKN-45 cells significantly reduced their colony formation ability (Fig. 3E, F). An immunofluorescence study showed that the proliferation marker Ki67 was significantly downregulated by FUT11 knockdown (Fig. 3G, H). Taken together, these data demonstrate that the downregulation of FUT11 inhibits the proliferation of GC cells.

Inhibition of FUT11 expression promotes ferroptosis in GC cells

There is a close relationship between ferroptosis and tumor growth [26]. However, it remains unclear whether

A

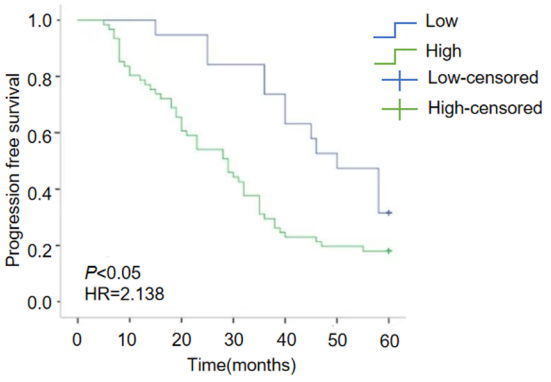

B

parameter	Univariate analysis		Multivariate analysis	
	F	*P*	*F*	*P*
Age	O.627	0.431	/	/
Gender	0.003	0.955	/	/
T	27.108	<0.001	5.385	0.024
N	19.800	<0.001	0.271	0.604
Grade	5.000	0.015	0.109	0.897
FUT11	23.318	<0.001	10.658	0.002

C

Clinicopathological characteristics	(-)	(+)	(++)	(+++)	χ^2	P
Age					0.124	0.725
<70	12	19	9	7		
>70	10	11	8	4		
Gender					1.899	0.168
Male	19	21	9	8		
Female	3	9	5	3		
Stage N					14.578	0.000
1	6	17	11	9		
0	16	13	6	2		
Stage T					9.410	0.002
T1-T2	17	14	8	6		
T3-T4	5	16	9	5		
Grade					5.539	0.063
High	2	2	1	0		
Moderate	10	6	4	4		
Low	10	22	12	7		

Fig. 2 The effect of relative expression level of FUT11 on 5-year survival rate after radical gastrectomy for GC. **A**. Kaplan survival analysis for the high expression and low expression FUT11 group. **B**. COX univariate and multivariate analysis of FUT11 expression with age, gender, differentiation level, and tumor TNM staging in GC patients. **C**.The relationship between the expression of FUT11 and clinicopathological characteristics in GC($n=80$)

FUT11 regulates ferroptosis in GC cells. To address this deficiency in the literature, we measured the concentrations of ROS, the lipid peroxidation marker 4-hydroxynonenal (4-HNE), and 4,4′-methylenedianiline (MDA) in HGC-27 and MKN-5 cells in which FUT11 had been knocked down, and found significantly higher concentrations of all three in both cell types (Fig. 4A–D). Moreover, TEM revealed significantly lower density of mitochondrial cristae, vacuolization of the mitochondrial matrix, and mitochondrial volume in cells in which FUT11 had been knocked down than in control cells (Fig. 4E). These findings suggest that the knockdown of FUT11 induces ferroptosis in GC cells.

Knocking down FUT11 induces ferroptosis in GC cells by reducing GPX4 expression

To further investigate the mechanism whereby FUT11 regulates ferroptosis in GC cells, we used GEPIA to analyze the relationship between FUT11 and mediators of ferroptosis in GC. Subsequently, we compared the expression of these molecules in GC cells in which FUT11 had been knocked down and control cells using qRT-PCR. We found that in FUT11-silenced GC cells, the expression of GPX4 was low, while that of SLC7A11, SLC3A2, TFRC, and ACSL4 were unaffected (Fig. 5A, B). It is well known that ferroptosis is induced by iron-dependent lipid peroxidation [27, 28]. However, GPX4

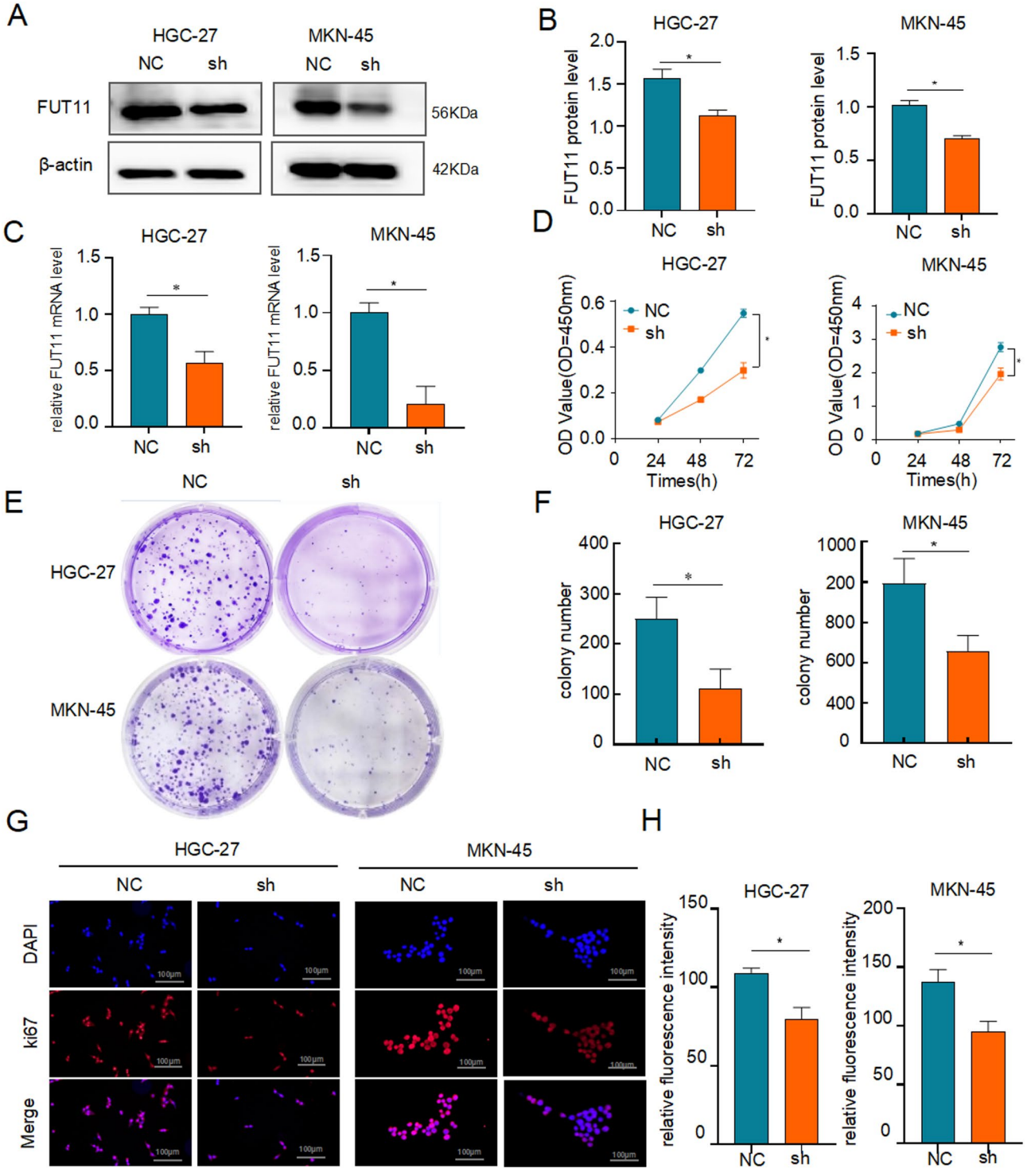

Fig. 3 Knockdown of FUT11 reduces the proliferation of GC cells. **A**, **B.** Western blots for the protein expression of FUT11 in the FUT11-silenced (sh) and control (NC) cells, with the results of grayscale analysis ($n = 3$). **C.** RT-qPCR-determined mRNA expression of FUT11 in FUT11-silenced (sh) and control (NC) cells. **D.** Proliferation of sh and NC cells, determined using a CCK-8 assay. **E**, **F.** Colony formation ability of sh and NC cells ($n = 3$). **G**, **H.** xpression of Ki67 in sh and NC cells, determined using the mean fluorescence intensity ($n = 3$). * $p < 0.05$ *versus* the corresponding control

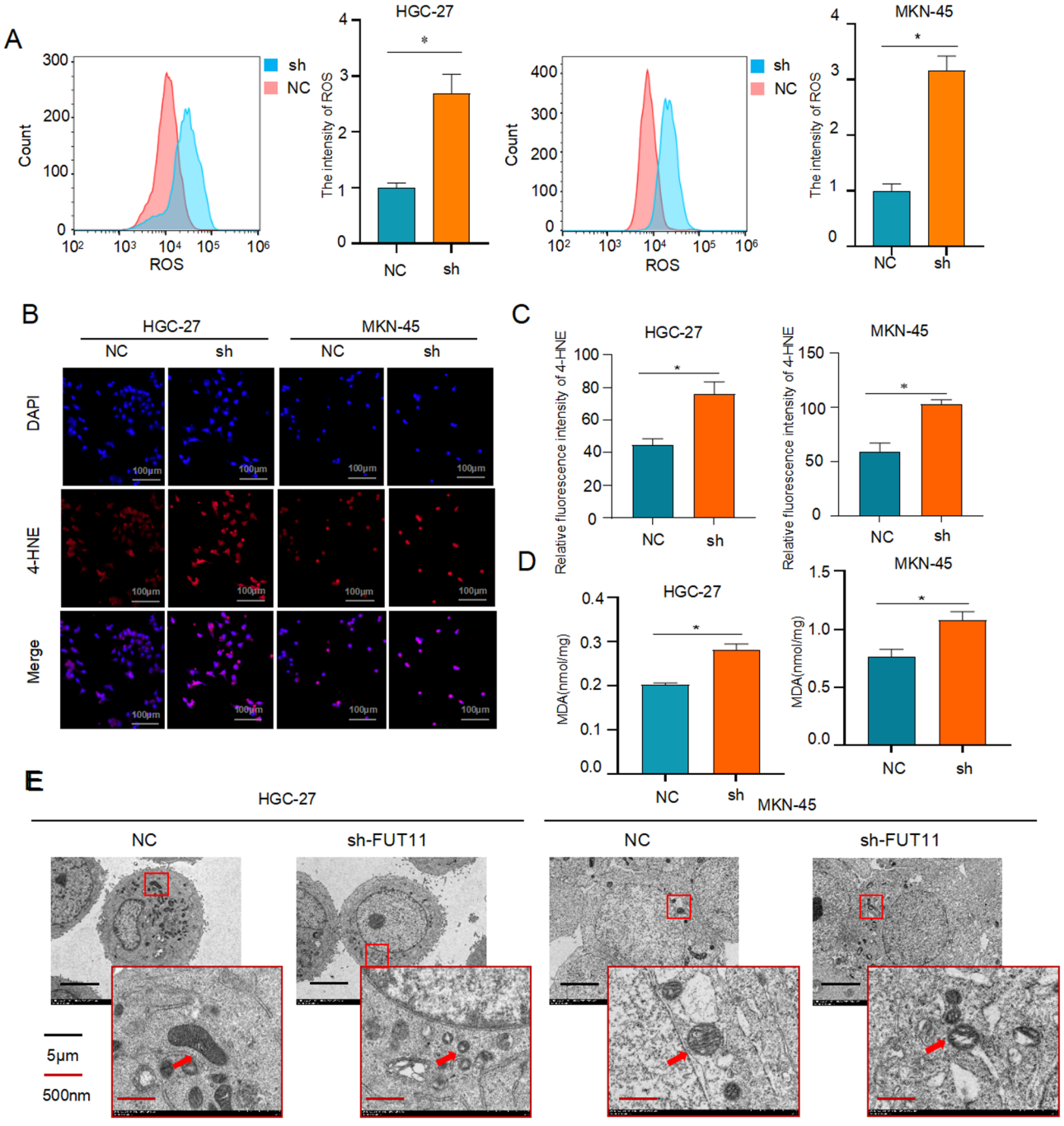

Fig. 4 Knockdown of FUT11 promotes ferroptosis in GC cells. **A.**ROS concentrations of FUT11-silenced (sh) and control (NC) cells, determined using flow cytometry ($n=3$). **B**, **C.** 4-HNE expression in sh and NC cells, determined using immunofluorescence ($n=3$). **D.** MDA content of sh and NC cells ($n=3$). **E.** Mitochondrial morphology of sh and NC cells. * $p<0.05$ *versus* the corresponding control

protects cells against ferroptosis by converting oxidized lipids into non-toxic alcohols [29, 30]. Using WB, we also showed that knocking down FUT11 reduces the protein expression of GPX4 in GC cells (Fig. 5C). Therefore, we speculated that FUT11 may promote ferroptosis in GC by regulating the expression of GPX4. To interrogate this hypothesis, we simultaneously overexpressed GPX4 in FUT11-silenced cells (Fig. 5D-F), which increased cell proliferation (Fig. 5G), and reduced the high ROS, 4-HNE, and MDA concentrations (Fig. 6A–G). In summary, the knockdown of FUT11 may induce ferroptosis in GC cells by reducing the expression of GPX4.

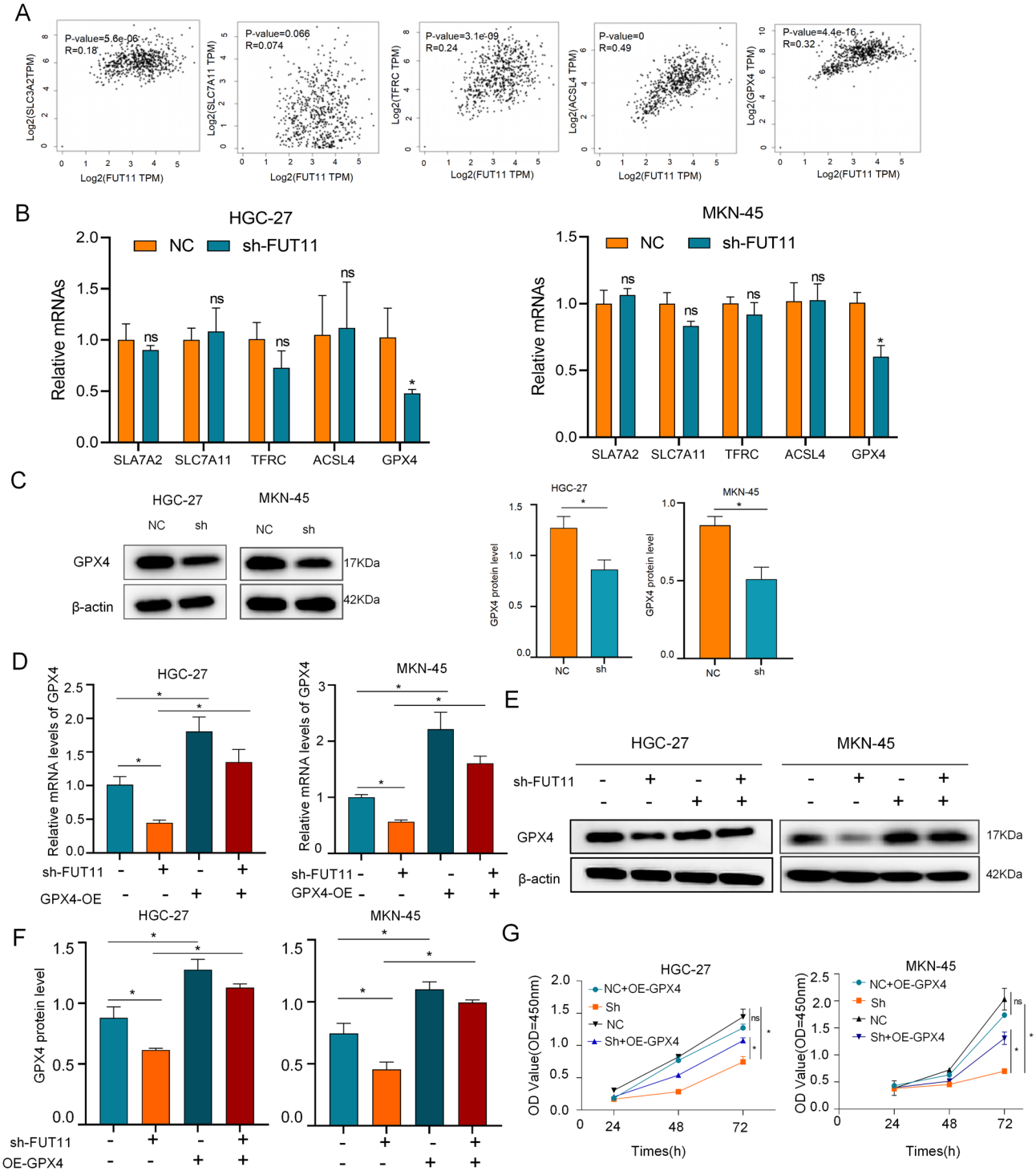

Fig. 5 FUT11 promotes ferroptosis in GC cells *via* GPX4. **A**.GEPIA analysis of the relationship between FUT11 and markers of ferroptosis. $P < 0.05$. **B.** mRNA expression of markers of ferroptosis in FUT11-silenced (sh) and control (NC) cells ($n = 3$). **C.** GPX4 protein expression in sh and NC cells, determined using western blotting, with the grayscale analysis ($n = 3$). **D.**mRNA expression of GPX4 in the control group (NC), FUT11 knockdown group (sh), GPX4 overexpression group (NC + GPX4-OE), and FUT11 knockdown + GPX4 overexpression group (Sh + GPX4-OE) of cells, measured using RT-qPCR. **E**, **F.** GPX4 protein expression in the control group (NC), FUT11 knockdown group (sh), GPX4 overexpression group (NC + GPX4-OE), and FUT11 knockdown + GPX4 overexpression group (sh + GPX4-OE) of cells, determined using western blotting, with the grayscale analysis ($n = 3$). **G.**Proliferative ability of the cells following the overexpression of GPX4, determined using a CCK-8 assay. * $p < 0.05$ *versus* the corresponding control

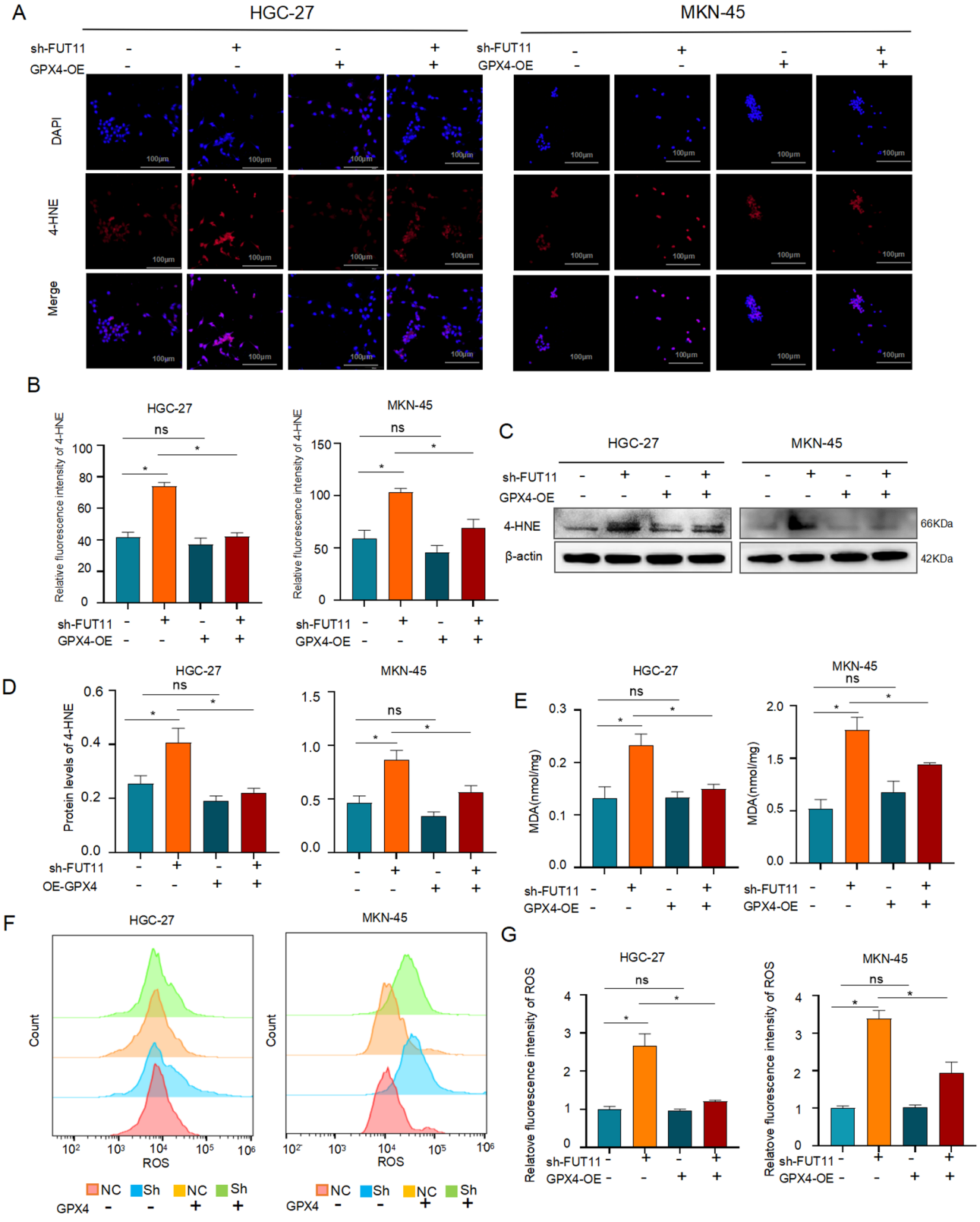

Fig. 6 Overexpression of GPX4 inhibits the effects of FUT11 knockdown. **A**, **B.** Expression of 4-HNE in the NC, sh, NC + GPX4-OE, and sh + GPX4-OE cells, determined using the mean fluorescence intensity ($n = 3$). **C**, **D** Protein expression of 4-HNE in the NC, sh, NC + GPX4-OE, and sh + GPX4-OE cells, determined using western blotting, with the grayscale analysis ($n = 3$). **E.** MDA concentrations in the NC, Sh, NC + GPX4-OE, and Sh + GPX4-OE cells ($n = 3$). **F**, **G.** ROS concentrations in the NC, Sh, NC + GPX4-OE, and Sh + GPX4-OE cells, determined using flow cytometry ($n = 3$). * $p < 0.05$ *versus* the corresponding control

FUT11 regulates the expression of GPX4 and promotes tumor growth in vivo

To investigate the role of the FUT11-GPX4 axis in GC development, we transfected MKN-45 cells with NC, sh-FUT11, NC + GPX4-OE, or sh-FUT11 + GPX4-OE, then subcutaneously injected these cells into groups of BALB/c nude mice. Three weeks later, the mice were euthanized and the sizes and masses of the subcutaneous tumors generated were measured. In this xenograft model, we found that knocking down FUT11 reduced GC proliferation, whereas the overexpression of GPX4 reversed this effect (Fig. 7A–C). WB and immunohistochemistry demonstrated that in tumors formed by sh-FUT11 GC cells, the expression of GPX4 was low, whereas that of 4-HNE was very high. However, the overexpression of GPX4 reduced the expression of 4-HNE (Fig. 7D, E). These findings collectively suggest that FUT11 regulates the proliferation of GC cells *via* GPX4.

Discussion

Gastric cancer is one of the most common malignancies of the digestive system, and despite its declining incidence, it remains one of the most common cancers worldwide and an important global health issue, owing to its high prevalence and associated mortality [31, 32]. Therefore, it is imperative to elucidate the molecular mechanisms underlying the development and progression of GC.

The results suggest that patients with high FUT11 expression have a poor prognosis and are associated with tumor stage and lymph node metastasis, especially those with higher TNM stage or poorer differentiation status.In vitro studies have found that FUT11 knockdown inhibits the proliferation of GC cells, which is consistent with the findings of Cao et al. [11]. However, the mechanisms whereby FUT11 regulates GC have not been identified. Here, we have shown that FUT11 knockdown increases the levels of ROS and lipid peroxidation in GC cells and causes specific changes in their mitochondria (a decrease in the number of mitochondrial crests, vacuolization of the mitochondrial matrix, and a reduction in volume). These results imply that the knockdown of FUT11 induces ferroptosis in GC cells. Subsequently, we used the GEPIA database analysis to establish that FUT11 expression positively correlates with that of GPX4. GPX4 has a catalytic activity that maintains membrane lipid bilayer homeostasis by attenuating lipid peroxide toxicity and plays a key role in the protection of cells against ferroptosis [33, 34]. RT-qPCR and WB analysis showed that reducing FUT11 expression significantly reduces the expression of GPX4, increases intracellular lipid peroxidation, and promotes ferroptosis in GC cells, and that the overexpression of GPX4 reduces ferroptosis in these cells. In summary, we have shown that FUT11 promotes the development and progression of GC by targeting GPX4 and thereby inhibiting ferroptosis.

We have revealed the relationship between FUT11 and ferroptosis for the first time in the present study, and this may lead to novel means of diagnosing and treating GC. However, we have not identified the specific mechanisms underpinning the relationship between FUT11 and GPX4. Previous studies have shown that fucosylation, a post-translational modification, mediates glycoprotein and glycolipid cell surface expression, trafficking, secretion, and quality control, and thereby regulates a variety of intercellular and intracellular signaling pathways [7, 35]. For example, the inhibition of fucosylation in breast cancer cells reduces the expression of functional E-selective ligands and growth factors and reduces the activation of the ERK1/2 and p38 pathways, resulting in reductions in cell proliferation and migration [36]. In addition, Cao et al. found that FUT11 promotes the proliferation and migration of GC cells through the PI3K/AKT pathway and inhibits the apoptosis of GC cells [11]. Therefore, we hypothesized that FUT11 may affect the activation of the epidermal growth factor receptor (EGFR) signaling pathway.

The EGFR signaling pathway is an intracellular signaling pathway that is typically ligand-activated and transmits information from the cell surface and intracellular vesicles to the nucleus, causing the transcription of genes encoding proteins responsible for cellular proliferation, growth, and differentiation [37, 38]. The classical EGFR signaling pathways, including the Ras/MAPK, PI3K/AKT, and phospholipase C (PLC)/protein kinase C (PKC) signaling pathways, play important roles in tumor proliferation, growth, and migration [37].

It has previously been shown that GPX4 is regulated by the EGFR signaling pathway. For example, P2RX7 regulates the expression of GPX4 through the MAPK/ERK pathway, which regulates ferroptosis in patients with epilepsy [39]. Furthermore, Angong Niuhuang Wan, a prescription from traditional Chinese medicine may affect ferroptosis through the PPARγ/AKT/GPX4 signaling pathway [40]. Therefore, it is reasonable to speculate that FUT11 may affect ferroptosis in GC through the EGFR signaling pathway, but this hypothesis requires testing.

A limitation of the present study is that we have only evaluated the relationship between FUT11 and ferroptosis, and therefore its relationships with autophagy, pyroptosis, and necrosis should be explored in the future.

Conclusion

Our study showed that patients with high expression of FUT11 had a poor prognosis and could inhibit ferroptosis in GC by increasing the expression of GPX4, thereby promoting tumor growth.

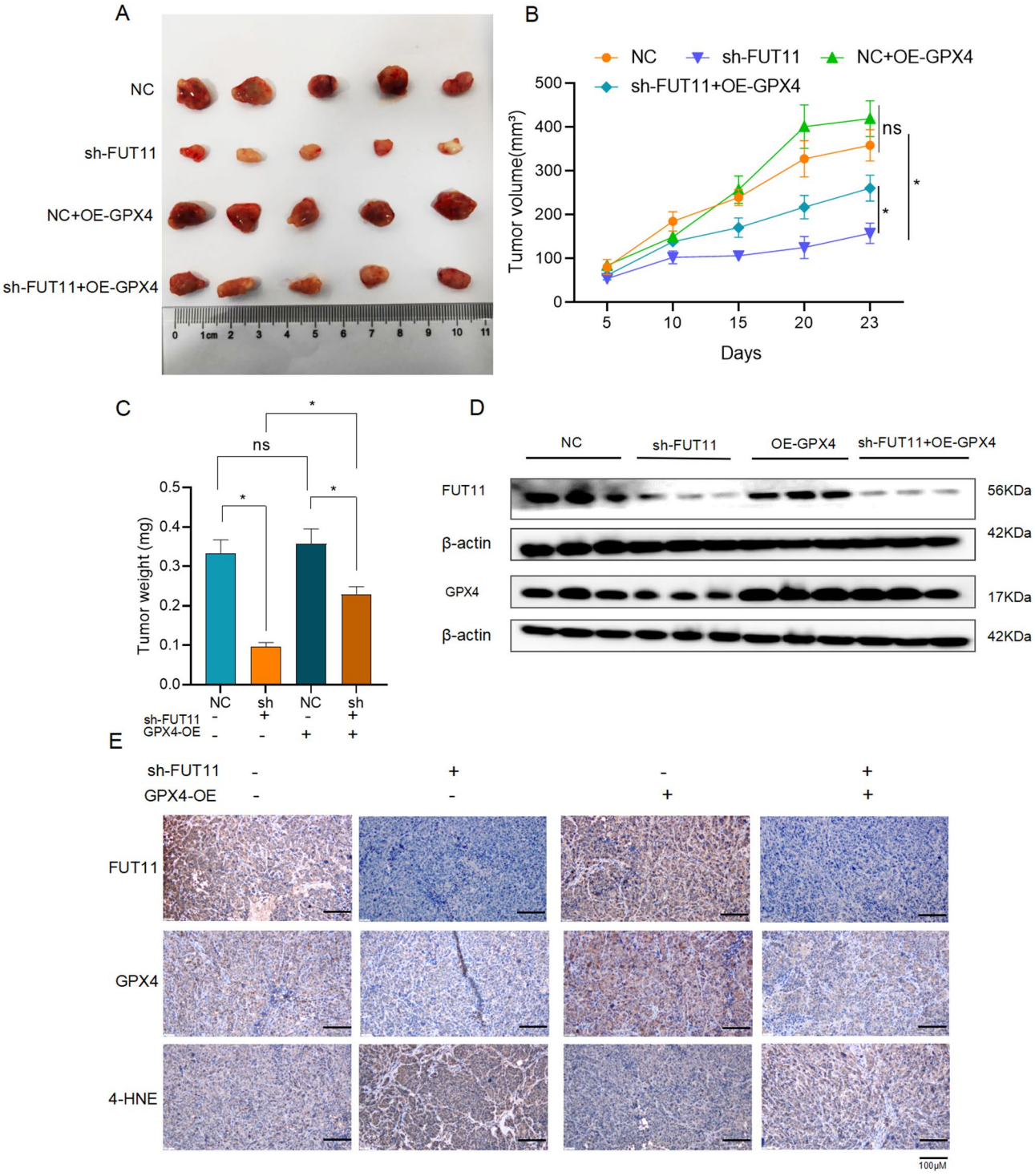

Fig. 7 FUT11 regulates the expression of GPX4 and promotes tumor growth *in vivo*.**A.** Images of tumors of the BALB/c nude mice ($n=5$). **B.** Tumor growth curve for each group ($n=5$). **C.** Tumor mass for each group ($n=5$). **D**. Protein expression of FUT11 and GPX4 in the xenograft tumors, assessed using western blot analysis. **E.** Protein expression of FUT11, GPX4, and 4-HNE in the xenograft tumors, assessed using immunofluorescence. *$P<0.05$ *versus* the corresponding control; ns, not significant

Supplementary Information

The online version contains supplementary material available at https://doi.org/10.1186/s12885-025-14340-4.

Supplementary Material 1

Author contributions

Bingbing Zhang wrote the main manuscript text and prepared Figs. 1, 2, 3, 4, 5 and 6. Yali Chen and Xue Zhou Gu prepared Figs. 1, 2 and 3. Yu Zheng prepared research ideas.Zhonghua Jiang prepared research ideas and funding. All authors reviewed the manuscript.

Funding

This work was supported by Natural Science Foundation of Jiangsu Province(grant no. BK20211116), the Science and Technology Development Fund of the Affiliated Hospital of Xuzhou Medical University(grant no. XYFM202304), Jiangsu University Medical Education Collaborative Innovation Fund (grant no. 2023105), Jiangsu Province Traditional Chinese medicine science and technology development program (grant no. YB2020079), Medical Research Project of Yancheng City Health Commission (grant no. YK2024012) and the Science and Technology Plan Project of Yancheng City (grant no. YCBK2024069).

Data availability

All data generated or analyzed in this study were included in the main document and supplementary information files of this article.Other source data that support the findings of this study are available from the corresponding author on reasonable request.

Declarations

Ethical approval

The protocol was approved by the Ethics Committee of the Yancheng Clinical College, Xuzhou Medical University based on the international ethics of this study developed in accordance with the 1964 Declaration of Helsinki(2023-K-095). The article involves animal experiments in which the tumor volume and the maximum tumor size of comply with the ethical requirements of the Animal Experimentation Center of Jiangsu Medical Vocational College. All institutional and national guidelines for the care and use of laboratory animals were followed (SYLL-2023-706).

Consent for publication

Not applicable.

Competing interests

The authors declare no competing interests.

Received: 12 July 2024 / Accepted: 15 May 2025
Published online: 22 May 2025

References

1. Siegel RL et al. Cancer Statistics, 2021. CA Cancer J Clin. 2021;71(1):7–33.
2. Guan WL, He Y, Xu RH. Gastric cancer treatment: recent progress and future perspectives. J Hematol Oncol. 2023;16(1):57.
3. Tan Z. Recent advances in the surgical treatment of advanced gastric cancer: A review. Med Sci Monit. 2019;25:3537–41.
4. Leng Q, et al. Fucosylation genes as Circulating biomarkers for lung cancer. J Cancer Res Clin Oncol. 2018;144(11):2109–15.
5. Liu B, et al. Correction: MiR-29b/Sp1/FUT4 axis modulates the malignancy of leukemia stem cells by regulating fucosylation via Wnt/beta-catenin pathway in acute myeloid leukemia. J Exp Clin Cancer Res. 2023;42(1):208.
6. Lin S, et al. Alpha-(1,6)-fucosyltransferase (FUT8) affects the survival strategy of osteosarcoma by remodeling TNF/NF-kappaB2 signaling. Cell Death Dis. 2021;12(12):1124.
7. Mueller TM, et al. Altered fucosyltransferase expression in the superior Temporal gyrus of elderly patients with schizophrenia. Schizophr Res. 2017;182:66–73.
8. Lin G, et al. Dynamic analysis of N-glycomic and transcriptomic changes in the development of ovarian cancer cell line A2780 to its three cisplatin-resistant variants. Ann Transl Med. 2020;8(6):289.
9. Zhang X, Wang Y. Identification of hub genes and key pathways associated with the progression of gynecological cancer. Oncol Lett. 2019;18(6):6516–24.
10. Zhang P, et al. Dry and wet experiments reveal the significant role of FUT11 in clear cell renal cell carcinoma. Int Immunopharmacol. 2022;113(Pt B):p109447.
11. Cao W, et al. Knockdown of FUT11 inhibits the progression of gastric cancer via the PI3K/AKT pathway. Heliyon. 2023;9(7):e17600.
12. Mu C, et al. The role of iron homeostasis in remodeling immune function and regulating inflammatory disease. Sci Bull (Beijing). 2021;66(17):p1806–1816.
13. Deng Q, et al. Low molecular weight fucoidan LF2 improves the immunosuppressive tumor microenvironment and enhances the anti-pancreatic cancer activity of oxaliplatin. Biomed Pharmacother. 2024;173:pe116360.
14. Tang D, et al. Ferroptosis: molecular mechanisms and health implications. Cell Res. 2021;31(2):107–25.
15. Jiang X, Stockwell BR, Conrad M. Ferroptosis: mechanisms, biology and role in disease. Nat Rev Mol Cell Biol. 2021;22(4):266–82.
16. Nie J, et al. Role of ferroptosis in hepatocellular carcinoma. J Cancer Res Clin Oncol. 2018;144(12):2329–37.
17. Xie Y, et al. The tumor suppressor p53 limits ferroptosis by blocking DPP4 activity. Cell Rep. 2017;20(7):1692–704.
18. Ishimoto T, et al. CD44 variant regulates redox status in cancer cells by stabilizing the xCT subunit of system xc(-) and thereby promotes tumor growth. Cancer Cell. 2011;19(3):387–400.
19. Greenshields AL, Shepherd TG, Hoskin DW. Contribution of reactive oxygen species to ovarian cancer cell growth arrest and killing by the anti-malarial drug Artesunate. Mol Carcinog. 2017;56(1):75–93.
20. Sun X, et al. HSPB1 as a novel regulator of ferroptotic cancer cell death. Oncogene. 2015;34(45):5617–25.
21. Hasegawa M, et al. Functional interactions of the cystine/glutamate antiporter, CD44v and MUC1-C oncoprotein in triple-negative breast cancer cells. Oncotarget. 2016;7(11):11756–69.
22. Guo J, et al. Ferroptosis: A novel Anti-tumor action for cisplatin. Cancer Res Treat. 2018;50(2):445–60.
23. Lu Y, et al. KLF2 inhibits cancer cell migration and invasion by regulating ferroptosis through GPX4 in clear cell renal cell carcinoma. Cancer Lett. 2021;522:1–13.
24. Li D, et al. CST1 inhibits ferroptosis and promotes gastric cancer metastasis by regulating GPX4 protein stability via OTUB1. Oncogene. 2023;42(2):83–98.
25. Shao CJ, et al. Downregulation of miR-221-3p promotes the ferroptosis in gastric cancer cells via upregulation of ATF3 to mediate the transcription Inhibition of GPX4 and HRD1. Transl Oncol. 2023;32:101649.
26. Lei G, Zhuang L, Gan B. Targeting ferroptosis as a vulnerability in cancer. Nat Rev Cancer. 2022;22(7):381–96.
27. Stockwell BR, et al. Ferroptosis: A regulated cell death Nexus linking metabolism, redox biology, and disease. Cell. 2017;171(2):273–85.
28. Dixon SJ, et al. Ferroptosis: an iron-dependent form of nonapoptotic cell death. Cell. 2012;149(5):1060–72.
29. Yang WS, et al. Regulation of ferroptotic cancer cell death by GPX4. Cell. 2014;156(1–2):317–31.
30. Ingold I, et al. Selenium utilization by GPX4 is required to prevent Hydroperoxide-Induced ferroptosis. Cell. 2018;172(3):409–e42221.
31. Lopez MJ, et al. Characteristics of gastric cancer around the world. Crit Rev Oncol Hematol. 2023;181:103841.
32. Petryszyn P, Chapelle N, Matysiak-Budnik T. Gastric Cancer: where Are We Heading? Dig Dis. 2020;38(4):280–5.
33. Zhang Y, et al. mTORC1 couples cyst(e)ine availability with GPX4 protein synthesis and ferroptosis regulation. Nat Commun. 2021;12(1):1589.
34. Wang S, et al. Molecular mechanisms of ferroptosis and its role in prostate cancer therapy. Crit Rev Oncol Hematol. 2022;176:103732.
35. Ma B, Simala-Grant JL, Taylor DE. Fucosylation in prokaryotes and eukaryotes. Glycobiology. 2006;16(12):158. R-184R.
36. Carrascal MA, et al. Inhibition of fucosylation in human invasive ductal carcinoma reduces E-selectin ligand expression, cell proliferation, and ERK1/2 and p38 MAPK activation. Mol Oncol. 2018;12(5):579–93.
37. Schlessinger J. Cell signaling by receptor tyrosine kinases. Cell. 2000;103(2):211–25.
38. Schlessinger J. Receptor tyrosine kinases: legacy of the first two decades. Cold Spring Harb Perspect Biol, 2014. 6(3).

39. Li X, et al. The microRNA-211-5p/P2RX7/ERK/GPX4 axis regulates epilepsy-associated neuronal ferroptosis and oxidative stress. J Neuroinflammation. 2024;21(1):13.
40. Bai X, et al. Angong Niuhuang Wan inhibit ferroptosis on ischemic and hemorrhagic stroke by activating PPARgamma/AKT/GPX4 pathway. J Ethnopharmacol. 2024;321:117438.

Publisher's note